The official journal of the Japan Atherosclerosis Society and
the Asian Pacific Society of Atherosclerosis and Vascular Diseases

Original Article

J Atheroscler Thromb, 2024; 31: 1460-1478. http://doi.org/10.5551/jat.64754

JNK Pathway-Associated Phosphatase Deficiency Facilitates Atherosclerotic Progression by Inducing T-Helper 1 and 17 Polarization and Inflammation in an ERK- and NF-κB Pathway-Dependent Manner

Xinjing Chen, Mingcheng Fang, Jingxuan Hong and Yansong Guo

Department of Cardiology, Provincial Clinical Medical College of Fujian Medical University, Fujian Institute of Cardiovascular Disease, Fujian Provincial Hospital, Fuzhou, China

Aim: JNK pathway-associated phosphatase (JKAP) regulates T cell-mediated immunity and inflammation, which are involved in atherosclerosis pathogenesis. This study investigated the effects of JKAP on T-helper (Th) cell polarization, inflammation, and atherosclerotic progression.

Methods: Serum JKAP levels were measured in 30 patients with coronary heart disease (CHD) and 30 controls. CHD blood naïve $CD4^+$ T cells were acquired, followed by JKAP overexpression and knockdown with or without treatment with PD98059 (ERK inhibitor) or BAY-11-7082 (NF-κB inhibitor) *in vitro*. $CD4^+$ T-cell conditional JKAP ablation mice were established *in vivo*, followed by the construction of an atherosclerosis model.

Results: JKAP was reduced and negatively correlated with the Gensini score, CRP, Th1 cells, Th17 cells, and proinflammatory cytokines in patients with CHD. *In vitro*, JKAP overexpression suppressed Th1 and Th17 cell differentiation and proinflammatory cytokines, whereas JKAP knockdown exerted the opposite effect; however, JKAP modification did not affect Th2 cell differentiation. Interestingly, JKAP negatively regulated the ERK and NF-κB pathways; meanwhile, the PD98059 and BAY-11-7082 treatments repressed Th1 and Th17 cell differentiation, and attenuated the effect of JKAP knockdown on these indices. *In vivo*, conditional $CD4^+$ T-cell JKAP ablation increased Th1 and Th17 cell polarization in the spleen, lymph node, blood, and/or aortic root. Furthermore, $CD4^+$ T-cell conditional JKAP ablation exaggerated atherosclerotic lesions in the aorta, elevated $CD4^+$ cell infiltration and proinflammatory cytokines in the aortic root, and activated the ERK and NF-κB pathways in the aortic root.

Conclusion: JKAP ablation facilitates atherosclerosis progression by promoting Th1 and 17 polarization and inflammation through regulation of the ERK and NF-κB pathways.

Key words: JKAP, Atherosclerosis progression, Th cells, Inflammation, ERK and NF-κB pathways

1. Introduction

Coronary heart disease (CHD) is a common cardiovascular disease that is the leading cause of global morbidity and mortality[1, 2]. Atherosclerosis is the major cause of CHD, and its risk factors include traditional factors, such as hypertension, hyperlipidemia, diabetes, obesity, and smoking as well as non-traditional factors such as physical inactivity, psychological distress, somnipathy, and air pollution[3-5]. As a chronic and complicated procedure, atherosclerosis is traditionally considered to be induced by lipid accumulation, endothelial dysfunction, inflammatory infiltration, and

Address for correspondence: Xinjing Chen, Department of Cardiology, Provincial Clinical Medical College of Fujian Medical University, Fujian Institute of Cardiovascular Disease, Fujian Provincial Hospital, 134 East Street, Fuzhou 350001, China E-mail: che58957152@163.com

Received: November 29, 2023 Accepted for publication: March 10, 2024

calcification or plaque formulation, etc[6-8].

Recently, the involvement of immunoinflammatory mechanisms in atherosclerosis has attracted increasing attentions[9]. For instance, macrophages harboring innate immune memory facilitate the atherosclerotic process by elevating the secretion of inflammatory cytokines, cholesterol deposition, and vascular smooth muscle cell dysfunction[10, 11] Macrophage-targeted therapy has been proposed as an option for atherosclerosis treatment[12]. Interestingly, T cell subsets are also closely involved in the pathogenesis of atherosclerosis by stimulating immunity, producing inflammatory cytokines, accumulating lipoproteins, and inducing plaques, especially $CD4^+$ T cells and $CD8^+$ T cells[13-15]. Among $CD4^+$ T cells, T-helper (Th) 1 and 17 cells act as proatherogenic roles by interacting with macrophages, dendritic cells, and endothelial cells via various cytokines; however, Th2 cells have an anti-atherogenic role, although the findings concerning these details remain controversial[16-18]. Encouragingly, a few recent studies have also shed light on the possibility of targeting Th1 or Th17 cells for atherosclerosis therapy[19, 20].

JNK pathway-associated phosphatase (JKAP), also known as dual-specificity phosphatase 22 (DUSP22), is a JNK activator that exerts multiple biological functions, including T-cell-mediated immunity, Th cell polarization, and inflammation[21-23]. For instance, it has been proposed that JKAP dephosphorylates the tyrosine[394] residue of Lck to suppress the T-cell receptor (TCR) signaling pathway, thus inhibiting immunity and inflammation[21]. Another interesting study revealed that JKAP knockdown in $CD4^+$ T cells from patients with inflammatory bowel disease induced the polarization of Th1 and Th17 cells[23]. Clinically, several studies have indicated that JKAP is associated with Th cell polarization and inflammation levels in various diseases, such as autoimmune, vascular ischemic, and geriatric diseases[24-27].

Given the above information, it is hypothesized that JKAP may be involved in the atherosclerosis process by regulating Th cell polarization and inflammation; however, related data have not been reported. Therefore, the current study investigated the effect of JKAP on Th cell polarization, inflammation, and atherosclerotic progression both *in vitro* and *in vivo*, as well as its interaction with the ERK and NF-κB pathways.

2. Methods

2.1. Patients and Samples

Thirty patients with CHD and 30 age-and sex-matched normal controls were enrolled. All patients were diagnosed using imaging examinations. Peripheral blood samples were acquired, and peripheral blood mononuclear cells (PBMCs) were isolated to detect the Th1/Th2/Th17 cell percentage using a Human Th1/Th2/Th17 Phenotyping Kit (BD Biosciences (Franklin Lakes, New Jersey, USA). Serum samples were used to assess the levels of JKAP, TNF-α, IL-6, IFN-γ, IL-4, and IL-17A using an enzyme-linked immunosorbent assay (ELISA) (Sangon Biotech, Shanghai, China).

Written informed consent was obtained from all participants. The study protocol was in accordance with the Declaration of Helsinki and was approved by the Ethics Committee. Another 15 CHD patients were enrolled, and their PBMCs and serum were collected to detect the JKAP mRNA relative expression in $CD4^+$ T cells and serum JKAP levels.

2.2. Human Naïve $CD4^+$ T-Cell Isolation and Adenovirus Transfection

A human naïve $CD4^+$ T-cell isolation kit (Miltenyi, Bergisch Gladbach, Germany) was used to isolate naïve $CD4^+$ T cells from the PBMCs of five CHD patients and three normal controls, according to the kit's instructions. In brief, PBMCs were isolated using density gradient medium (Solarbio, Beijing, China) for 10 min ($800 \times g$). We then incubated the PBMCs with naive $CD4^+$ T Cell Biotin-Antibody Cocktail II at 4℃ for 5 min. The PBMCs were then incubated with naïve $CD4^+$ T cell MicroBead Cocktail II for 10 min at 4℃. Finally, PBMCs were applied to a column in a magnetic field, and the cells that passed through the column (representing enriched naïve $CD4^+$ T cells). Subsequently, the cells were subjected to T-cell culture in expansion medium (Takara, Tokyo, Japan). JKAP-overexpressing adenovirus (Ad-JKAP), JKAP-knockdown adenovirus (Ad-shJKAP), or control adenovirus (Scramble) (Genepharma, Shanghai, China) was then transfected into these cells according to the manufacturer's instructions. The transfected naïve $CD4^+$ T cells were harvested after 48 h of incubation, followed by reverse transcription-quantitative polymerase chain reaction (RT-qPCR) and Western blotting.

2.3. Th1/Th2/Th17 Cell Polarization

Naïve human $CD4^+$ T-cell isolated from CHD patients and normal controls were polarized as described previously[28, 29]. In brief, transfected cells were seeded in 24-well plates at a density of 1×10^5 cells/well and stimulated under different conditions. Specifically, Th1 polarization was performed with IL-12 (10 ng/mL; Sigma, Santa Fe, New Mexico,

USA) and anti–IL-4 (1:200; Affinity, Liyang, China), Th2 polarization was conducted using IL-4 (5 ng/mL; Sigma) and anti–IFN-γ (1:200; Affinity), and Th17 polarization was accomplished with TGF-β (10 ng/mL; Sigma), IL-23 (10 ng/mL; Sigma), IL-1β (10 ng/mL; Sigma), IL-6 (10 ng/mL; Sigma), anti–IFN-γ (1:200) and anti–IL-4 (1:200). After stimulation for three days, the cells and supernatants were separately analyzed by flow cytometry and ELISAs.

2.4. PD98059 and BAY-11-7082 Treatment

Human naïve $CD4^+$ T cells isolated from CHD patients were seeded in a 24-well plate at a density of 1×10^5 cells/well, following transfection with Ad-shJKAP or scrambled adenovirus as indicated. PD98059 (MEK/ERK inhibitor, 20 μM; Sigma)[30] and BAY-11-7082 (NF-κB inhibitor, 10 μM; Sigma)[31] were added. Western blot assays were performed after 48 h. Th1/Th17 polarization assays were performed in the presence of PD98059 or BAY-11-7082. Cells and supernatants were isolated separately for flow cytometry and ELISAs after three days of incubation.

2.5. Animals

Conditional JKAP ablation mice ($JKAP^{fl/fl}CD4^{Cre}$) were created with a CRE recombinase-based system by crossbreeding $JKAP^{fl/fl}$ mice with $CD4^{Cre}$ mice. $JKAP^{fl/fl}$ littermates were used as the controls. Subsequently, $JKAP^{fl/fl}CD4^{Cre}$ and $JKAP^{fl/fl}$ mice were backcrossed with $Apoe^{-/-}$ transgenic C57BL/6 mice. For atherosclerosis experiments, 8-week-old $JKAP^{fl/fl}CD4^{Cre}$ mice (n=6) and $JKAP^{fl/fl}$ mice (n=6) were fed a high-fat diet for 12 weeks. Normal C57BL/6 mice (n=6) fed a regular diet were used as the normal wild-type (WT) group. The mice were anesthetized by isoflurane inhalation (1.5-2%) and euthanized by cervical dislocation. PBMC samples were collected, and a $CD4^+$ T-cell isolation kit (BD Biosciences) was used to isolate $CD4^+$ and $CD4^-$ cells for the assessment of JKAP expression by RT-qPCR and Western blotting. Serum samples were used for ELISA detection. Aorta samples were collected for RT-qPCR, histological analyses, and immunohistochemical staining. $CD4^+$ T cells in the lesions of the aortic root were isolated using a $CD4^+$ T-cell isolation kit (BD Biosciences) and used for Western blot assays. The details of $CD4^+$ T cell isolation were as follows: first, the plaque was minced with a surgical razor blade and digested with enzyme mix (400 U/mL Collagenase I [MCE, Shanghai, China], 60 U/mL DNase I [MCE], 10 U/mL Collagenase XI [Sigma], and 60 U/mL hyaluronidase [Yeasen, Shanghai, China]) at 37℃ for 40 min, and the cell suspension was filtered through a 70-μm strainer. Subsequently, the cells were washed with 1X BD IMag™ buffer incubated with anti-mouse CD4 Magnetic Particles at 4℃ for 30 min. The tube was then placed on a Cell Separation Magnet for 6 min, followed by aspiration and discarding of the supernatant. Finally, the cells were washed and collected in phosphate-buffered saline (PBS) with a tube on the Cell Separation Magne. Spleen and lymph node (inguinal and axillary) samples were collected to determine the Th1/Th2/Th17 cell percentage by flow cytometry.

The Animal Care and Use Committee approved the animal experimental protocols.

2.6. Histology and Immunohistochemistry (IHC) Staining

Whole-aorta samples were fixed with 4% polyformaldehyde and stained using Oil Red O staining solution (Beyotime, Shanghai, China) according to the kit's protocol. Aortic root samples were fixed, embedded, and cut into 4 μm-thick sections. For evaluation of tissue morphology, the sections were stained with H&E staining solution (Beyotime). A Picrosirius red staining kit (Beyotime) was used to detect collagen fibers. For IHC staining, sections were incubated with primary antibodies, secondary antibodies, and DAB staining solution (Beyotime). Sections were observed under a light microscope (Olympus, Tokyo, Japan). Images were analyzed using the ImageJ software program (NIH, Bethesda, Maryland, USA). Regarding nonspecific positivity, a negative control was set, and evaluations were made.

2.7. Flow Cytometry

A Human or Mouse Th1/Th2/Th17 Phenotyping Kit (BD Biosciences) was used to determine Th cell percentages. Single-cell suspensions from the spleen and lymph nodes were prepared as in a previous study[32]. In brief, cells were incubated with Fc-receptor block (BD Biosciences) for 20 min at 4℃ and subsequently stained with specific antibodies for 0.5 h at 4℃. For flow cytometry of PBMCs or naïve $CD4^+$ T cells, cells were stimulated with phorbol myristic acetate (PMA; 1 μM; Beyotime), ionomycin (5 μM; Sigma), and BD GolgiStop (1 μL/mL; BD Biosciences) for 4 h before collection and stained with specific antibodies for 0.5 h at 4℃. FACSCanto II (BD Biosciences) was used to detect the samples, and the FlowJo 7.6 software program (FlowJo, Ashland, Kentucky, USA) was used for data analyses.

2.8. ELISAs

The levels of JKAP, total cholesterol (TC), low-density lipoprotein cholesterol (LDL-C), total

triglyceride (TG), TNF-α, IL-6, IFN-γ, IL-4, and IL-17A in the serum or cell supernatants were measured using commercial kits (Sangon, Solarbio, or EIAab [Shanghai, China]) according to the manufacturer's instructions. In brief, the samples were incubated in a microplate that had been precoated with specific antibodies. Subsequently, the samples were incubated with a biotin-conjugated antibody, HRP-conjugated streptavidin, and a chromogenic substrate. Finally, a microplate reader (Thermo Fisher, Waltham, Massachusetts, USA) was used to measure absorbance (OD) at 450 nm.

2.9. RT-qPCR

Total RNA from the indicated cells and tissues was purified using TRIzol (Invitrogen, Waltham, Massachusetts, USA) and quantified using a NanoDrop (Thermo Fisher). RT-qPCR was performed using a cDNA synthesis kit (Beyotime) and PCR Mix (Beyotime). The relative expression of JKAP, IFNG, IL4, and IL17A was normalized to that of GAPDH using the $2^{-\Delta\Delta Ct}$ method: $2^{-\{[Ct\ (interested\ gene\ of\ treated\ group) - Ct\ (GAPDH\ of\ treated\ group)] - [Ct\ (interested\ gene\ of\ control\ group) - Ct\ (GAPDH\ of\ control\ group)]\}}$. Primers used are listed in **Supplementary Table 1**.

2.10. Western Blotting

Total protein was extracted using RIPA buffer (Sigma) and quantified using a BCA kit (Beyotime). Proteins were separated by sodium dodecyl sulfate-polyacrylamide gel electrophoresis (SDS-PAGE) in the presence of 10% precast gels (Beyotime) and then transferred onto polyvinylidene difluoride membranes (Beyotime). After blocking with 5% BSA solution for 1 h at 37℃, the membranes were subsequently incubated with primary antibodies for 1 h at 37℃ and secondary antibodies for 1 h at 37℃. The blots were then visualized using an ECL kit (Yeason, Shanghai, China). The antibodies used are listed in **Supplementary Table 2**.

2.11. Statistical Analyses

GraphPad Prism (GraphPad Software Inc., San Diego, California, USA) was used for statistical analyses and graphs. The correlation of the JKAP level with clinical characteristics was calculated using Spearman's rank correlation test. The normality and equal variances of data was checked by Shapito-Wilk test and Brown-Forsythe test, respectively. The parametric test was conducted when data were normally distributed with equal variances; otherwise, the nonparametric test was performed. The comparison was analyzed using an unpaired *t*-test (parametric), Mann-Whitney test (nonparametric), one-way analysis of variance (ANOVA) followed by Tukey's multiple comparisons test (parametric), or Kruskal-Wallis test followed by Dunn's multiple comparisons test (nonparametric). A P value <0.05 was considered to indicate significance.

3. Results

3.1. Clinical Implications of JKAP in CHD Patients

JKAP was reduced in CHD patients compared to controls ($P<0.001$) **(Fig. 1A)** but negatively correlated with the degree of stenosis, as reflected by the Gensini score ($P=0.019$), and the degree of inflammation, as reflected by the CRP level ($P=0.012$) **(Fig. 1B-C)**. Regarding the correlation of JKAP with Th cells, a negative correlation was found for JKAP with Th1 cells ($P=0.022$) and Th17 cells ($P=0.042$); however, it was not correlated with Th2 cells **(Fig. 1D-F)**. Regarding their secreted cytokines, JKAP had a negative correlation with IFN-γ ($P=0.033$) and a correlating trend with IL-17A ($P=0.069$) but not IL-4 **(Fig. 1G-I)**. The correlation of JKAP with inflammatory cytokines was investigated, which revealed that JKAP was negatively correlated with TNF-α ($P=0.005$) and a trend with IL-6 ($P=0.070$) **(Fig. 1J-K)**. In addition, serum JKAP levels were positively correlated with the relative JKAP expression in $CD4^+$ T cells in CHD patients ($P=0.036$) **(Supplementary Fig. 1)**.

3.2. The Effect of JKAP on CHD Th1 and Th17 Cell Polarization

Naïve $CD4^+$ T cells were acquired from CHD patients and modified with JKAP. The data showed that Ad-JKAP elevated ($P<0.001$) and Ad-shJKAP reduced the JKAP mRNA level in naïve $CD4^+$ T cells ($P<0.05$) **(Fig. 2A)**, which was confirmed by JKAP blotting and then was modified accordingly (both $P<0.05$) **(Fig. 2B-C)**. Thus, JKAP modification was considered to have been successful in these cells.

JKAP-modified CHD-naïve $CD4^+$ T cells were then polarized toward Th1/2/17 and evaluated by flow cytometry **(Fig. 2D)**. Ad-JKAP inhibited $CD4^+$ $IFN\text{-}\gamma^+$ cells and $CD4^+IL17A^+$ cells (both $P<0.05$) but did not affect $CD4^+IL4^+$ cells; conversely, Ad-shJKAP enhanced $CD4^+IFN\text{-}\gamma^+$ cells and $CD4^+$ $IL17A^+$ cells (both $P<0.05$) but showed no effect on $CD4^+IL4^+$ cells **(Fig. 2E)**. Simultaneously, specific cytokines released by Th1/2/17 cells were detected in the supernatant of JKAP-modified naïve $CD4^+$ T cells to further verify the above data. Ad-JKAP reduced IFN-γ ($P<0.05$) and IL-17A ($P<0.05$) levels but not IL-4 levels, while Ad-shJKAP increased IFN-γ ($P<$

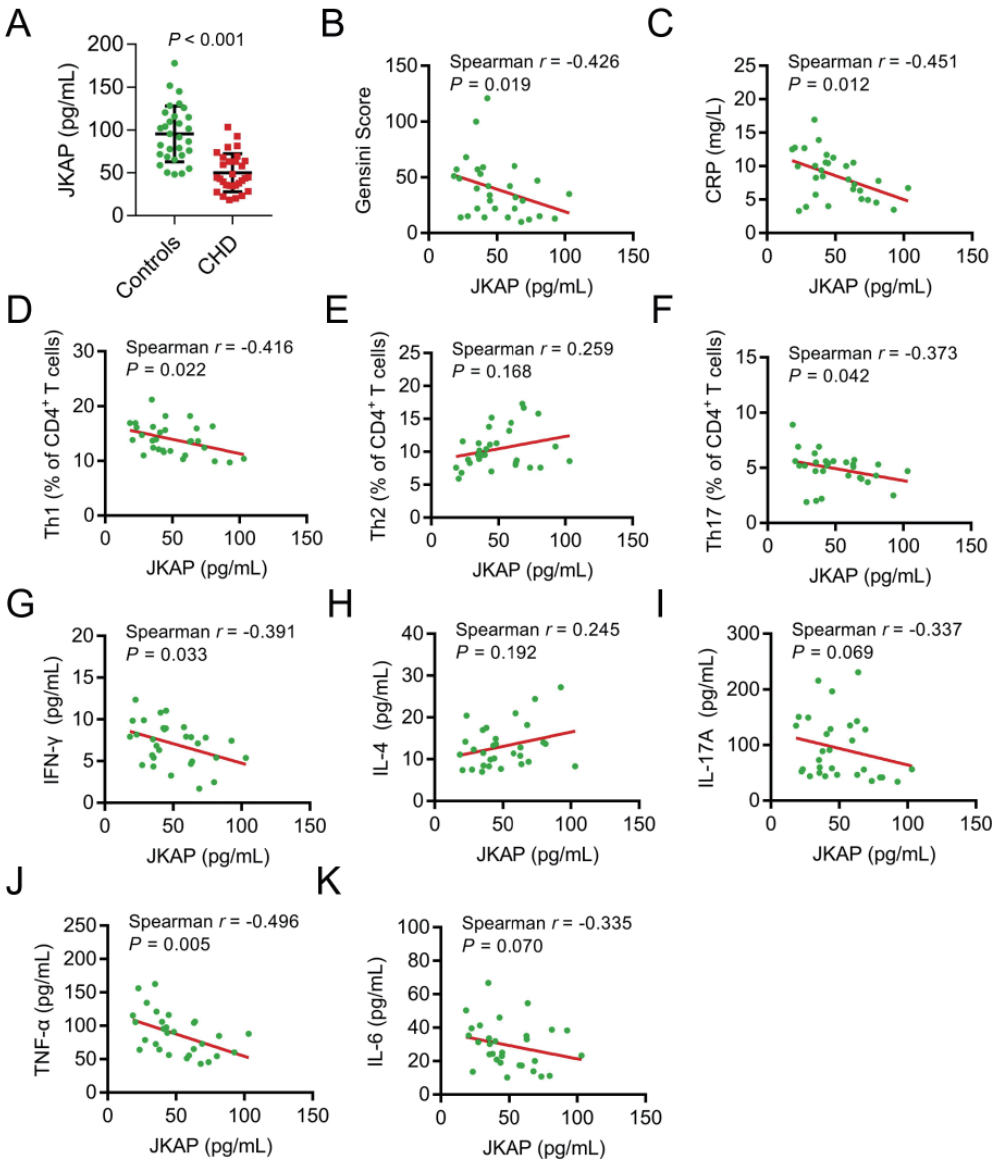

Fig. 1. Clinical implication of JKAP in CHD

The comparison of JKAP levels between patients with CHD ($n=30$) and those without CHD ($n=30$) (A); the correlation of JKAP levels with the Gensini Score (B), CRP (C), Th1 cells (D), Th2 cells (E), Th17 cells (F), IFN-γ (G), IL-4 (H), IL-17A (I), TNF-α (J), and IL-6 (K) in CHD patients ($n=30$). The upper and bottom line represent the 3/4 and 1/4 quartiles of JKAP in graph A, respectively; the middle line represents the median value of JKAP in graph A.

0.05) levels but not IL-17A or IL-4 levels **(Fig. 2F)**.

Interestingly, the effect of JKAP modification on age-matched control $CD4^+$ T cell differentiation was investigated. The JKAP expression was upregulated by Ad-JKAP but downregulated by Ad-shJKAP, indicating transfection success **(Supplementary Fig. 2A-C)**. Ad-JKAP decreased the numbers of $CD4^+$ IFN-γ^+ and $CD4^+IL17A^+$ cells and IFN-γ levels (all $P<0.05$), but did not affect $CD4^+IL4^+$ cells, IL-4 levels, or IL-17A levels **(Supplementary Fig. 2D-E)**. Ad-shJKAP increased the numbers of $CD4^+$IFN-γ^+ cells and IFN-γ levels (both $P<0.05$) but did not influence $CD4^+IL4^+$ cells, $CD4^+IL17A^+$ cells, IL-4 levels, or IL-17A levels **(Supplementary Fig. 2D-E)**.

3.3. The Effect of JKAP on the ERK and NF-κB Pathways in CHD Naïve $CD4^+$ T Cells

Next, Western blotting was conducted on JKAP-modified CHD-naïve $CD4^+$ T cells to detect the phosphorylation of ERK, p38, and IκBα **(Fig. 3A)**. Quantification revealed that Ad-JKAP suppressed ERK, p38, and IκBα phosphorylation (all $P<0.05$),

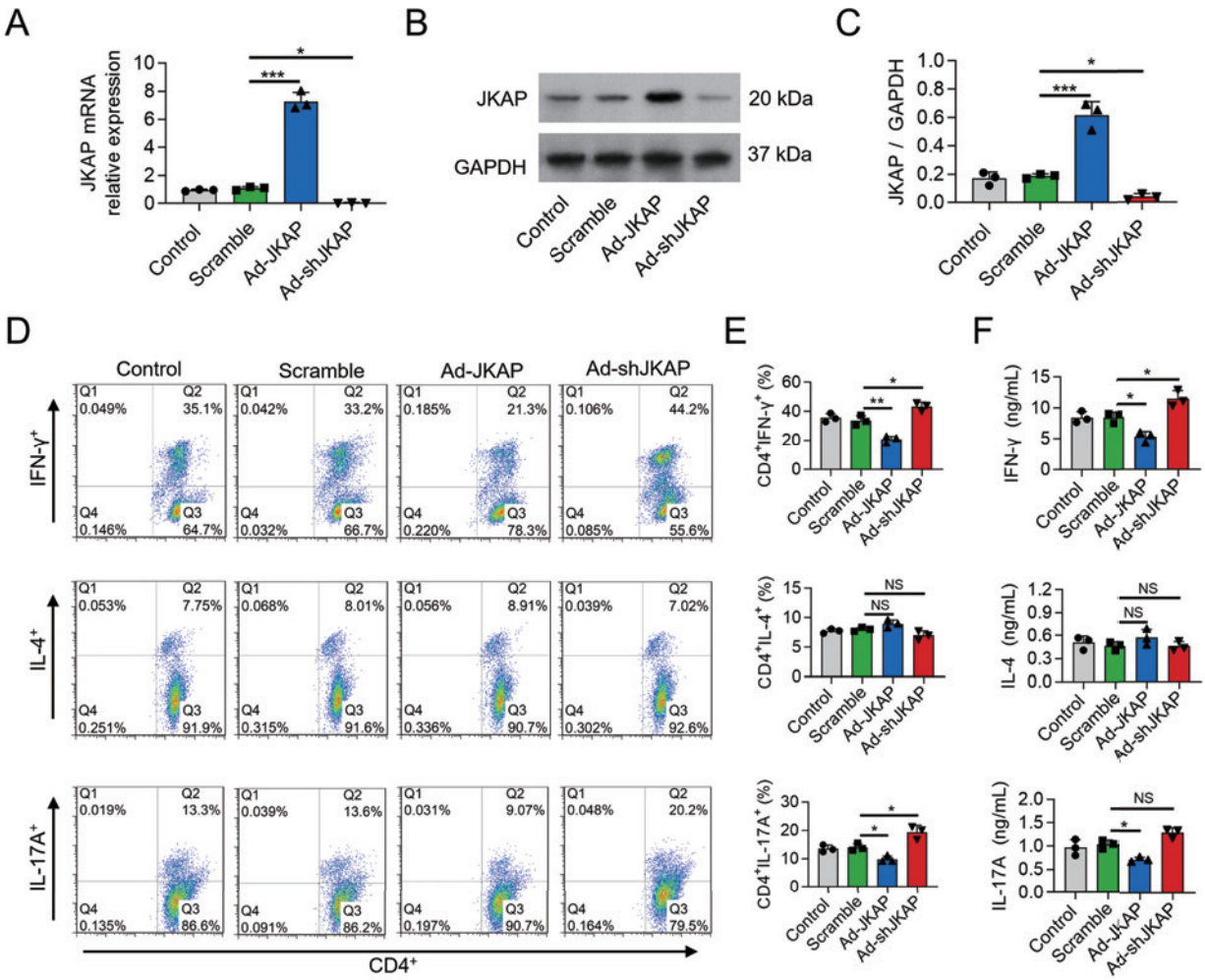

Fig. 2. The effect of JKAP on Th cell polarization from CHD naïve CD4⁺ T cells

The comparison of the JKAP mRNA expression ($n=3$) (A) and protein expression ($n=3$) (B, C); the comparison of Th1 cells, Th2 cells and Th17 cells ($n=3$) (D, E); the comparison of IFN-γ, IL-4 and IL-17A (F) after transfection ($n=3$). NS: not significant; * $P<0.05$; **: $P<0.01$; *** $P<0.001$. The bars represent the mean values, and error bars represent the standard deviations.

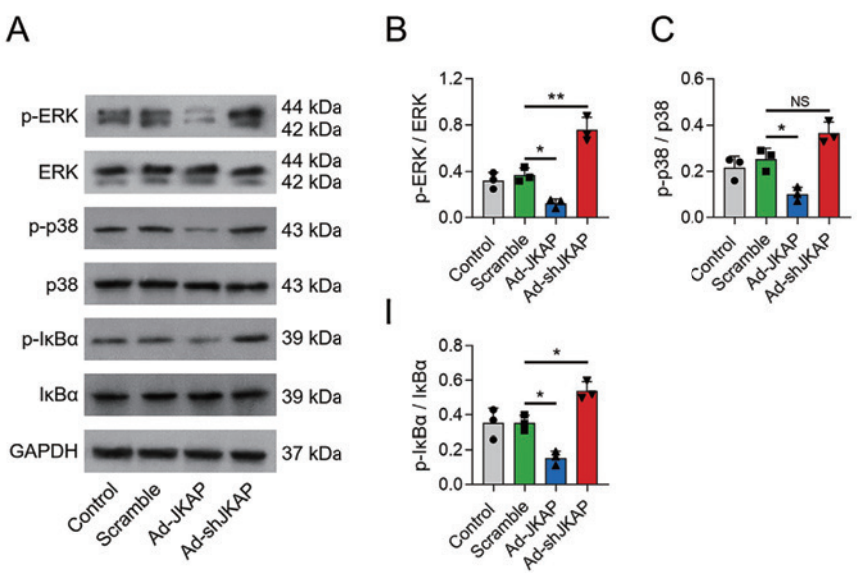

Fig. 3. The effect of JKAP on the ERK, p38, and NF-κB pathways in CHD naïve CD4⁺ T cells

The detection of ERK, p38, and IκBα and their phosphorylated proteins by Western blotting after transfection ($n=3$) (A); the comparison of the phosphorylation levels of ERK (B), p38 (C), and IκBα (D) after transfection ($n=3$). NS: not significant; *: $P<0.05$; **: $P<0.01$. The bars represent the mean values, and error bars represent the standard deviations.

whereas Ad-shJKAP elevated ERK and IκBα phosphorylation (both $P<0.05$) but did not affect p38 phosphorylation ($P>0.05$) **(Fig. 3B-D)**. Therefore, the ERK and NF-κB pathways were selected for further evaluations.

3.4. Involvement of the ERK and NF-κB pathways in JKAP's regulation of CHD Th cell polarization

Two chemical inhibitors of ERK (PD98059) and NF-κB (BAY-11-7082) were separately administered to Ad-shJKAP-affected CHD-naïve $CD4^+$ T cells. A Western blot analysis **(Fig. 4A)** revealed that neither PD98059 nor BAY-11-7082 affected the JKAP expression **(Fig. 4B)**. In addition, PD98059 suppressed ERK phosphorylation and attenuated the effect of Ad-shJKAP on ERK phosphorylation (both $P<0.01$) **(Fig. 4C)**. At the same time, BAY-11-7082 repressed IκBα phosphorylation and impaired Ad-shJKAP's effect on IκBα phosphorylation (both $P<0.01$) **(Fig. 4D)**.

Subsequently, Th cell polarization was assessed in Ad-shJKAP-affected CHD-naïve $CD4^+$ T cells, with or without PD98059 and BAY-11-7082, followed by flow cytometry **(Fig. 4E)**. Interestingly, it was observed that PD98059 not only directly reduced $CD4^+$IFN-γ^+ cells and supernatant IFN-γ levels but also weakened the effect of Ad-shJKAP on the above indices (all $P<0.05$); however, PD98059 had little effect on $CD4^+$ $IL17A^+$ cells and supernatant IL17A levels **(Fig. 4F-I)**. Furthermore, BAY-11-7082 decreased $CD4^+$IFN-γ^+ cells, $CD4^+IL17A^+$ cells, supernatant IFN-γ levels, and IL17A levels and attenuated the impact of Ad-shJKAP on these indices (all $P<0.05$) **(Fig. 4F-I)**

3.5. The Effect of Conditional JKAP Ablation in $CD4^+$ T Cells on Atherosclerosis Progression in Atherosclerotic Mice

After the construction of the atherosclerotic mouse model, blood JKAP levels were decreased in model mice compared to WT mice ($P<0.05$) **(Supplementary Fig. 3A)**. Furthermore, in blood $CD4^+$ T cells, JKAP expression was lower but p-ERK, p-p38, and p-IκBα expression was higher in model mice than in WT mice (all $P<0.05$) **(Supplementary Fig. 3B-C)**.

Next, conditional JKAP ablation mice ($JKAP^{fl/fl}CD4^{Cre}$) were generated. RT-qPCR revealed that the JKAP mRNA expression was reduced in $CD4^+$ T cells of $JKAP^{fl/fl}CD4^{Cre}$ mice vs. control mice ($P<0.001$), while the JKAP mRNA expression in $CD4^-$ T cells showed no change between these two groups **(Supplementary Fig. 4A)**; Western blot assays also showed a similar trend **(Supplementary Fig. 4B-C)**. In addition, serum JKAP levels were lower in $JKAP^{fl/fl}CD4^{Cre}$ mice than in control mice ($P<0.05$) **(Supplementary Fig. 5A)**. TC ($P<0.05$) and LDL-C ($P<0.05$) were higher in $JKAP^{fl/fl}CD4^{Cre}$ mice than in control mice, whereas TG only showed a tendency to be higher in $JKAP^{fl/fl}CD4^{Cre}$ mice than in control mice, but the difference was not statistically significant ($P=0.061$) **(Supplementary Fig. 5B-D)**.

Subsequently, an atherosclerosis model was constructed in $JKAP^{fl/fl}CD4^{Cre}$ and control mice. The aorta samples of these mice were stained with Oil Red O to indicate atherosclerotic lesions **(Fig. 5A)**, which showed that the atherosclerotic lesion area was larger in $JKAP^{fl/fl}CD4^{Cre}$ mice than in the control mice ($P<0.01$) **(Fig. 5B)**. Hematoxylin-Eosin (H&E) staining, picrosirius red staining, and IHC staining were conducted in the aortic root samples **(Fig. 5C)**, which showed that the area of atherosclerotic lesions ($P<0.05$) **(Fig. 5D)** and collagen fiber content in the lesion ($P<0.01$) **(Fig. 5E)** were both increased in $JKAP^{fl/fl}CD4^{Cre}$ mice compared to control mice; however, the $JKAP^+$ area was reduced in the lesion of $JKAP^{fl/fl}CD4^{Cre}$ mice compared to control mice ($P<0.05$) **(Fig. 5F)**. In addition, the $CD68^+$ area was increased ($P<0.05$), indicating a higher level of macrophage infiltration in $JKAP^{fl/fl}CD4^{Cre}$ mice than in control mice **(Fig. 5G)**, and the α-SMA^+ area showed a tendency to increase but was not statistically significant ($P=0.078$), suggesting a higher level of endothelial hyperplasia in $JKAP^{fl/fl}CD4^{Cre}$ mice than in control mice **(Fig. 5H)**.

3.6. The Effect of Conditional JKAP Ablation in $CD4^+$ T Cells on Th1 and Th17 Polarization in Atherosclerotic Mice

The spleens and lymph nodes of the mice were acquired for Th cell detection. In the spleen, $CD4^+$ IFN-γ^+ ($P<0.01$) and $CD4^+IL\text{-}17A^+$ ($P<0.05$) cells were higher, while $CD4^+IL\text{-}4^+$ cells remained unchanged in $JKAP^{fl/fl}CD4^{Cre}$ mice compared to control mice **(Fig. 6A-B)**. However, in the lymph nodes, a similar trend in the above cell percentages was found between the two groups **(Fig. 6C-D)**. Furthermore, in the serum, IFN-γ was increased ($P<0.05$), and IL-17A showed an increasing tendency but did not reach statistical significance ($P=0.150$), whereas IL-4 levels did not differ between $JKAP^{fl/fl}CD4^{Cre}$ mice and control mice **(Fig. 6E)**. In the aorta, IFN-γ ($P<0.01$) and IL-17A ($P<0.05$) mRNA levels were elevated, but IL-4 mRNA levels were not markedly different between $JKAP^{fl/fl}CD4^{Cre}$ mice and control mice **(Fig. 6F)**.

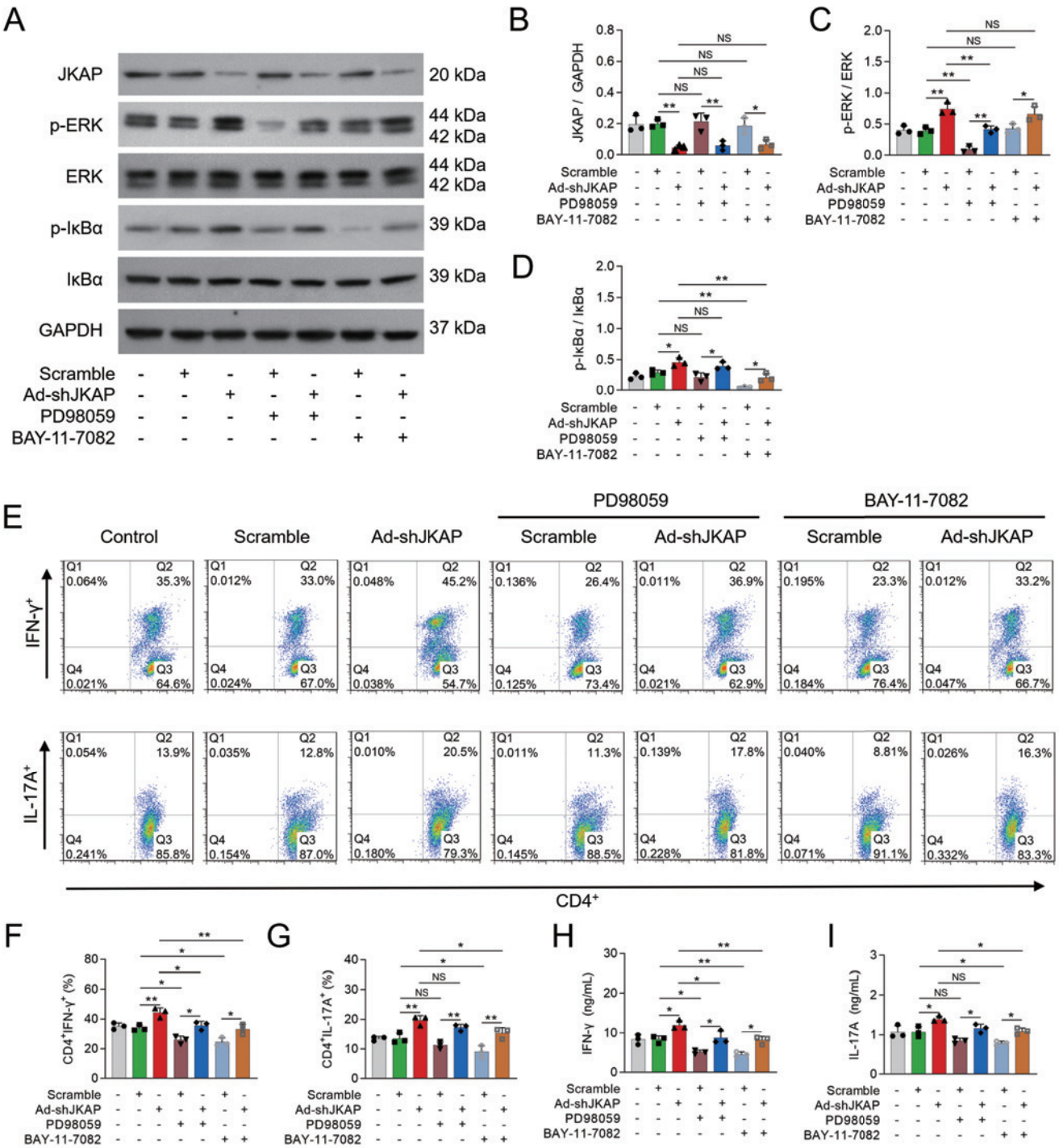

Fig. 4. The effect of ERK and NF-κB inhibitors on JKAP regulation of CHD Th cell polarization

The detection of JKAP, p-ERK, ERK, p-IκBα and IκBα by Western blot in JKAP-modulated cells with or without PD98059/BAY-11-7082 treatment ($n=3$) (A); comparison of JKAP (B), p-ERK/ERK (C) and p-IκBα/IκBα (D) in JKAP-modulated cells with or without PD98059/BAY-11-7082 treatment ($n=3$); Th1 and Th17 cell detection by flow cytometry in JKAP-modulated cells with or without PD98059/BAY-11-7082 treatment ($n=3$) (E); the comparison of Th1 cells (F), Th17 cells (G), IFN-γ (H) and IL-17A (I) in JKAP-modulated cells with or without PD98059/BAY-11-7082 treatment ($n=3$). NS: not significant; *: $P<0.05$; **: $P<0.01$. The bars represent the mean values, and error bars represent the standard deviations.

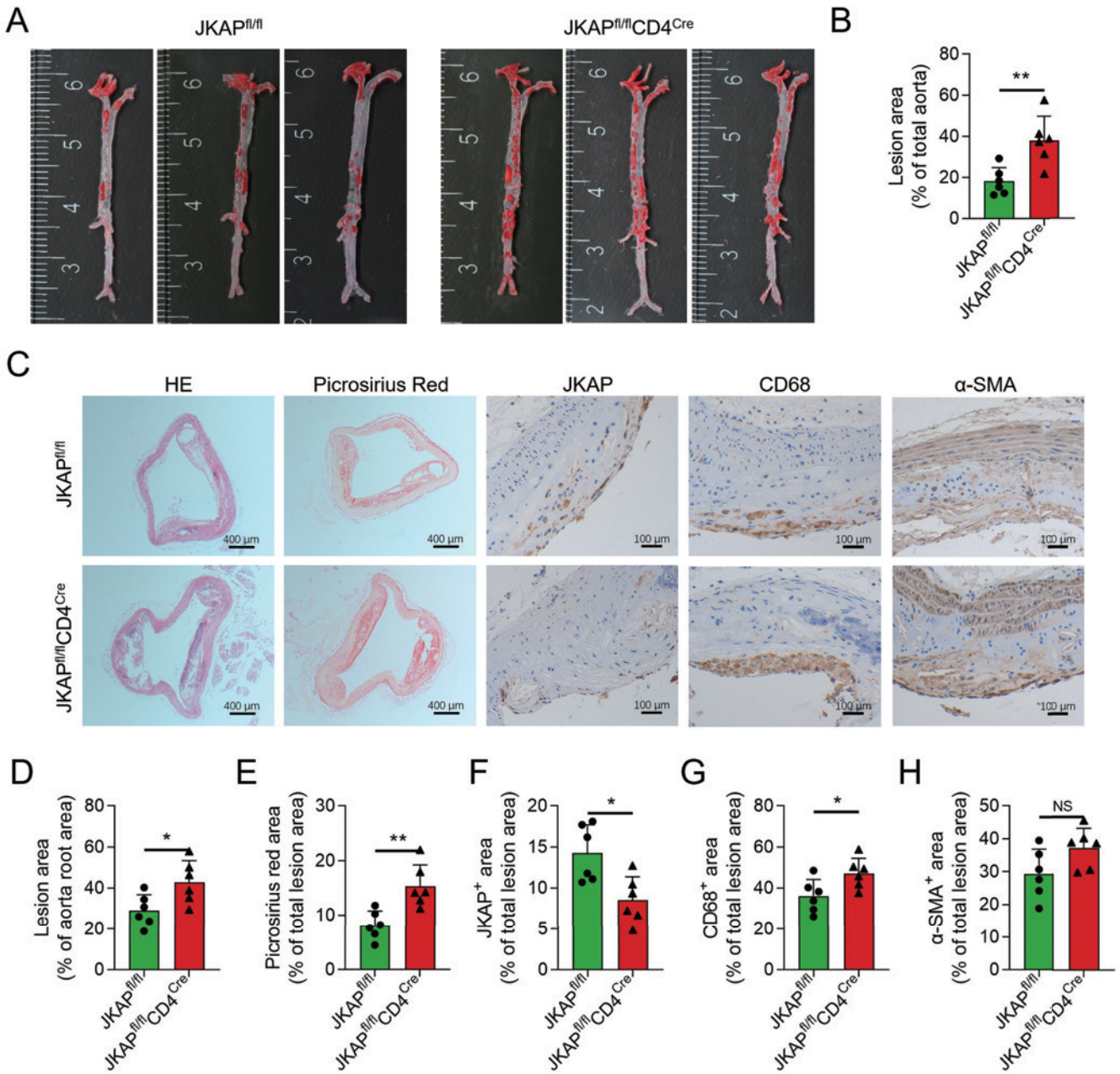

Fig. 5. Atherosclerotic lesions in JKAP$^{fl/fl}$CD4^{Cre} mice

The detection of atherosclerosis lesions in the aorta by Oil Red O staining ($n=6$) (A); the comparison of lesion area of total aorta ($n=6$) (B); H&E staining, picrosirius red staining and IHC assay in the aorta root ($n=6$) (C); the comparison of lesion area of aorta root area ($n=6$) (D); the comparison of picrosirius red area (E) JKAP$^+$ area (F), CD68$^+$ area (G) and α-SMA$^+$ area (H) of total lesion area ($n=6$). NS: not significant; *: $P<0.05$; **: $P<0.01$. The bars represent the mean values, and error bars represent the standard deviations.

3.7. The Effect of Conditional JKAP Ablation in CD4$^+$ T Cells on CD4$^+$ T Cell Infiltration and Inflammation in Atherosclerotic Mice

The levels of CD4$^+$ T-cell infiltration and inflammatory cytokines in the aorta root samples of the mice were evaluated by an IHC assay (Fig. 7A). CD4 was mainly expressed on T cells; therefore, the proportion was relatively low, while the other five inflammatory cytokines were mainly secreted by macrophages or lymphocytes, and some were expressed in endothelial cells and smooth muscle cells. The number of CD4$^+$ cells was elevated in JKAP$^{fl/fl}$CD4^{Cre} mice compared to control mice ($P<0.05$) (Fig. 7B). Meanwhile, proinflammatory cytokine-positive areas,

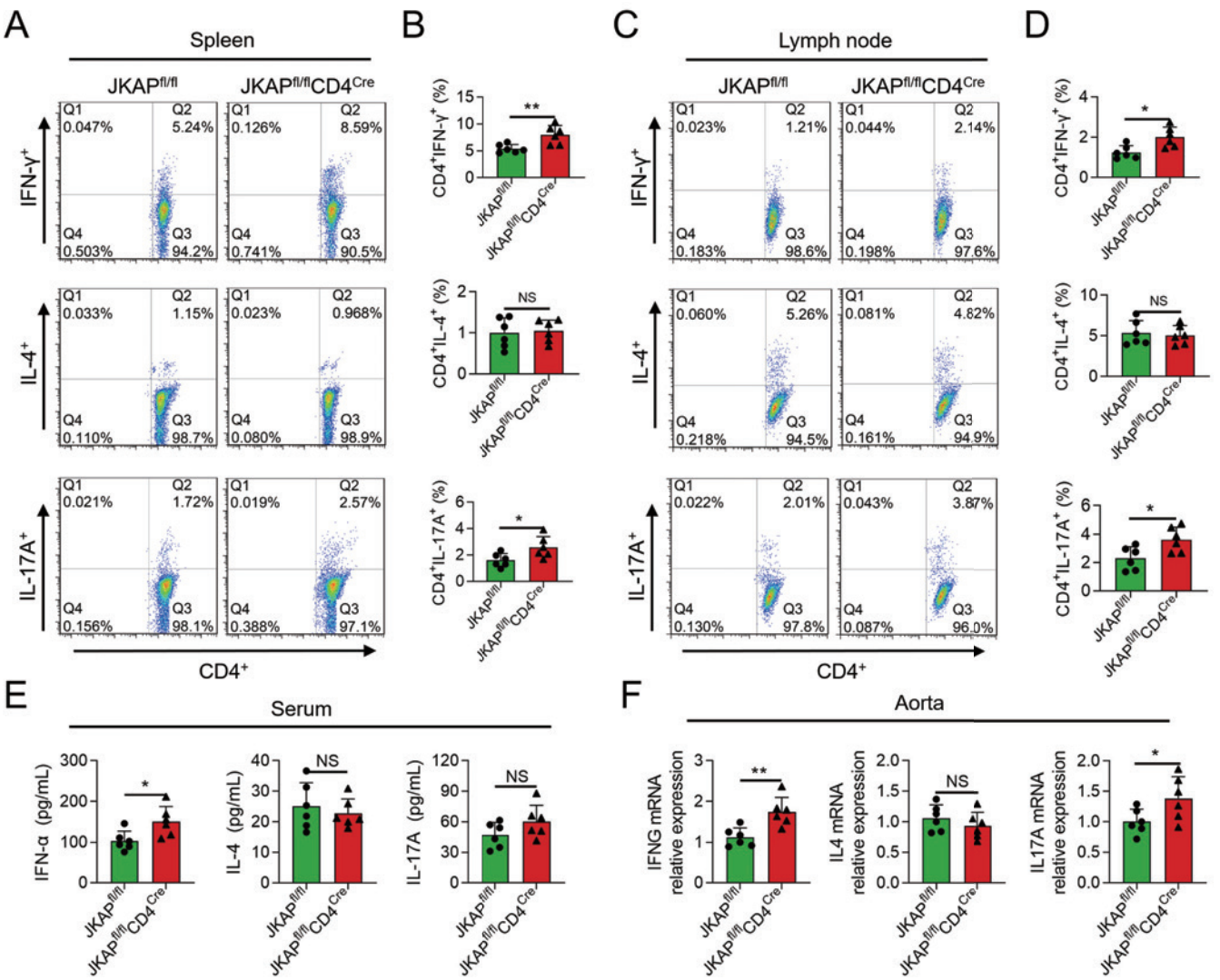

Fig. 6. Th cells in JKAP$^{fl/fl}$CD4^{Cre} mice

The comparison of Th1, Th2 and Th17 cells in the spleen ($n=6$) (A, B) and in the lymph node ($n=6$) (C, D); the comparison of IFN-γ, IL-4 and IL-17A in the serum ($n=6$) (E) and in the aorta ($n=6$) (F). NS: not significant; *: $P<0.05$; **: $P<0.01$. The bars represent the mean values, and error bars represent the standard deviations.

including TNF-α^+ and IL-6^+ areas, were both increased in JKAP$^{fl/fl}$CD4^{Cre} mice compared to control mice (both $P<0.05$) **(Fig. 7C-D)**. In addition, the IFN-γ^+ and IL-$17A^+$ areas were increased (both $P<0.05$), while the IL-4^+ area remained similar **(Fig. 7E-G)** in JKAP$^{fl/fl}$CD4^{Cre} mice compared to control mice.

3.8. The Effect of Conditional JKAP Ablation in CD4$^+$ T Cells on the ERK and NF-κB Pathways in Aortic Root Lesions in Atherosclerotic Mice

Phosphorylation of ERK, p38, and IκBα was also examined in the aorta root samples of the mice by IHC **(Fig. 8A)**. The proteins were mainly expressed in endothelial cells, smooth muscle cells, and lymphocytes, and some were expressed in macrophages and foam cells. The data showed that the p-ERK^+ **(Fig. 8B)** and p-$p38^+$ **(Fig. 8C)** areas were increased (both $P<0.05$), and the p-IκBα$^+$ area showed a predominant elevation ($P<0.01$) **(Fig. 8D)** in JKAP$^{fl/fl}$CD4^{Cre} mice compared with control mice. CD4$^+$ T cells in the lesions were then separated using flow cytometry, and the expression of p-ERK, p-p38, and p-IκBα was detected. As shown in **Supplementary Fig. 6A-B**, p-ERK and p-p38 expression was higher in JKAP$^{fl/fl}$CD4^{Cre} mice than in JKAP$^{fl/fl}$ mice (both $P<0.05$), but p-IkBα exhibited a tendency to be higher (but not statistically significant)

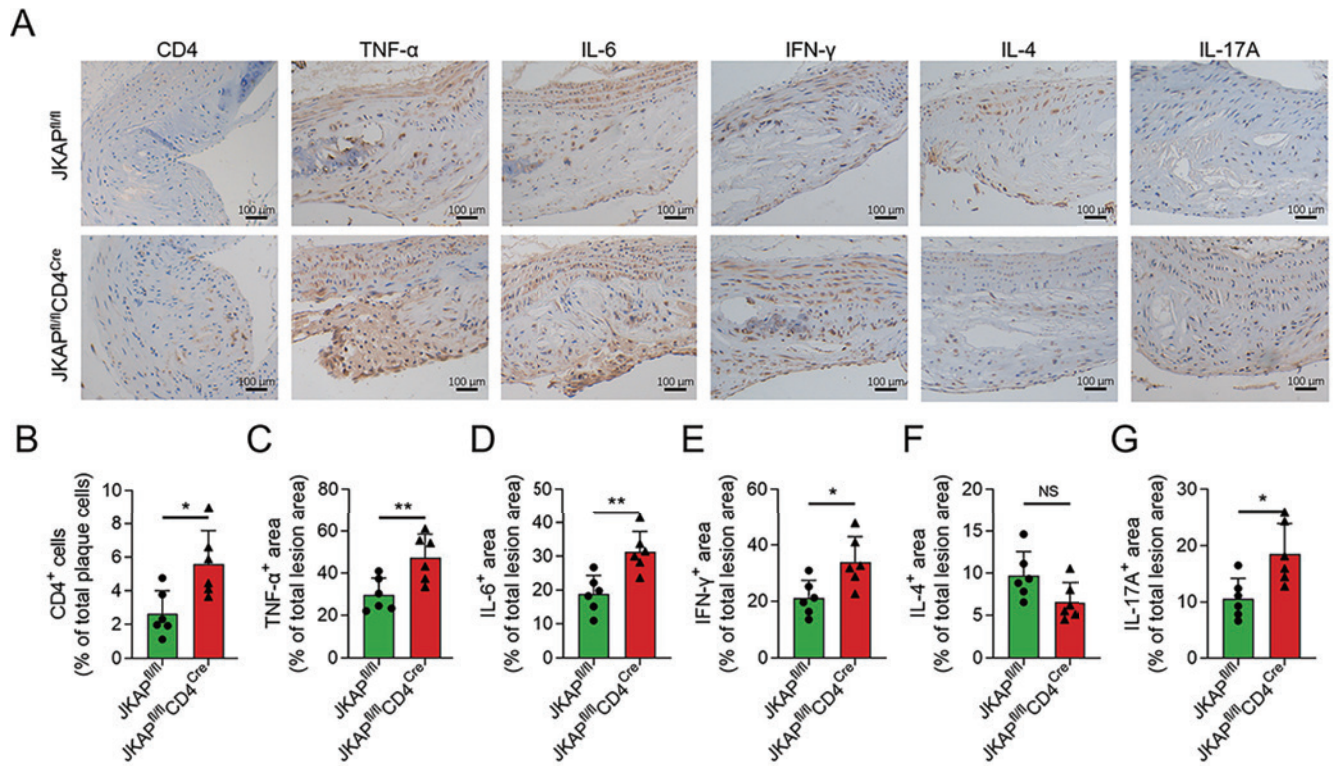

Fig. 7. $CD4^+$ cells and inflammatory cytokines in $JKAP^{fl/fl}CD4^{Cre}$ mice

The detection of $CD4^+$ cells and inflammatory cytokines in the aorta by an IHC assay ($n=6$) (A); the comparison of $CD4^+$ cells of total cells in the plaque ($n=6$) (B); the comparison of TNF-α^+ area (C), IL-6^+ area (D), IFN-γ^+ area (E), IL-4^+ area (F) and IL-$17A^+$ area (G) of total lesion area ($n=6$). NS: not significant; *: $P<0.05$; **: $P<0.01$. The bars represent the mean values, and error bars represent the standard deviations.

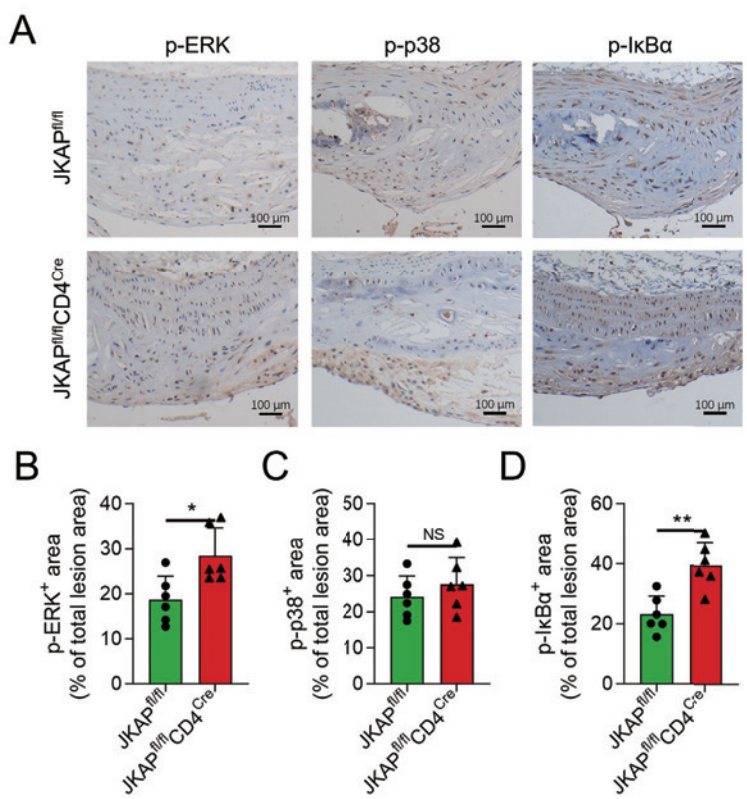

Fig. 8. ERK, p38, and NF-κB pathways in $JKAP^{fl/fl}CD4^{Cre}$ mice

The detection of the phosphorylation levels of ERK, p38, and IκBα in the aorta by IHC assay ($n=6$) (A); the comparison of the phosphorylation levels in the ERK^+ area (B), $p38^+$ area (C), and IκBα^+ area (D) of the total lesion area ($n=6$). NS: not significant; *: $P<0.05$; **: $P<0.01$. The bars represent the mean values, and error bars represent the standard deviations.

in $JKAP^{fl/fl}CD4^{Cre}$ mice than in $JKAP^{fl/fl}$ mice (P=0.136).

4. Discussion

$CD4^+$ T cells are critically involved in atherosclerosis and CHD. Clinically, it has been proposed that the proportion of Th17 cells and the Th17/Th1 ratio are elevated in patients with CHD compared to healthy subjects[33]. Other studies have indicated that dysregulated $CD4^+$ T cells with different phenotypes, including insufficient CD31-expressing, $IL10^+$, and apolipoprotein B-specific $CD4^+$ T cells, are observed in CHD patients[34-36]. From a laboratory perspective, an interesting study revealed that Th17 cell infiltration is observed from the early stage to the late stage of atherosclerosis, and neutralization of IL-17A hampers atherosclerosis progression in $Apoe^{-/-}$ mice fed a high-fat diet[37], and inhibition of $CD4^+$ T-cell polarization lowers the progression of atherosclerosis[38]. Furthermore, homocysteine-activated $CD4^+$ T cells increase pyruvate kinase muscle isozyme 2, a critical rate-limiting enzyme of glycolysis, thus accelerating atherosclerosis[39]. As mentioned earlier, JKAP modulates $CD4^+$ T-cell polarization through TCR signaling pathways, implying that JKAP might participate in the progression of atherosclerosis and CHD. In the current study, data from 30 CHD patients and 30 controls revealed that a decrease in JKAP was observed in CHD patients; meanwhile, in CHD patients, JKAP was negatively correlated with the degree of stenosis, inflammation, and Th1 and Th17 cells. One possible explanation for these findings is that a low JKAP expression can promote Th1 and Th17 cell polarization, which further accelerates the CHD pathogenesis and progression and induces inflammation[21, 22]. Regarding the source of JKAP in the blood, we considered that it might have resulted from lymphocyte and spleen flow. We referred to The Human Protein Atlas database (www.proteinatlas.org) and observed that various cells in the peripheral blood could produce JKAP, including T cells, B cells, granulocytes, and monocytes. In addition, we suspected that the reduced blood concentration of JKAP might result from increased immune-response activation and inflammation spread, especially TCR signaling-related effects.

To further verify this hypothesis, naïve $CD4^+$ T cells were sampled from patients with CHD, and JKAP was modulated in these cells. According to the flow cytometry data, JKAP overexpression suppressed Th1 and Th17 cell polarization, whereas JKAP knockdown exerted the opposite effect; however, JKAP modulation had no notable effect on Th2 cell polarization among CHD-naïve $CD4^+$ T cells. The Th1-, Th2-, and Th17-specific cytokines detected by an ELISA also confirmed these findings. One possible explanation may be that JKAP overexpression might suppress TCR signaling, thus inhibiting the polarization of Th1 and Th17 cells in CHD patients[21, 23] In addition, a previous study reported that JKAP is not correlated with Th2 cells[40], which is partly in line with our findings that JKAP does not affect Th2 cell polarization.

TCR signaling is a fundamental pathway that regulates multiple cellular functions of T cells, such as cell proliferation, polarization, migration, cytokine generation, and apoptosis, which is consistent with several vital pathways, such as the MEK/ERK pathway, p38/MAPK pathway, and NF-κB pathway[41]. According to previous studies, JKAP modulates Lck to suppress TCR signaling and thus participates in immunity and inflammation[21, 23]. Therefore, the current study further explored whether or not JKAP regulates the polarization of Th cells through the ERK, p38, and NF-κB pathways. A Western blot analysis showed that JKAP negatively regulates the ERK and NF-κB pathways in CHD $CD4^+$ T cells. By using chemical inhibitors of these pathways separately, it was confirmed that the ERK pathway is essential for JKAP regulation of Th1 polarization and that the NF-κB pathway is essential for JKAP regulation of Th1 and Th17 polarization.

The current study also conducted $CD4^+$ T cell conditional JKAP ablation in atherosclerotic mice. Compared with conventional knockout, conditional JKAP ablation was able to better verify the effect of $CD4^+$ T-cell JKAP on atherosclerosis and CHD progression, which is one of the highlights of this study.

The *in vivo* experiments revealed several interesting findings. First, the atherosclerotic lesion area was increased by conditional $CD4^+$ T-cell JKAP ablation, and collagen fiber, macrophage infiltration, and endothelial hyperplasia were elevated by $CD4^+$ T-cell conditional JKAP ablation, which are hallmarks of atherosclerosis[42-44]. However, the $JKAP^+$ area in the aortic root was reduced in the conditional JKAP-ablated mice. We deduced that $CD4^+$ T-cell infiltration was higher in conditional JKAP ablation mice than control mice, because these mice presented more severe atherosclerotic symptoms[45]; however, JKAP was knocked out in $CD4^+$ T cells. Thus, the aortic root of $JKAP^{fl/fl}CD4^{Cre}$ mice might have a lower level of JKAP. Second, an elevation in Th1 and Th17 cells was observed in the secondary lymph organs, spleen, and lymph nodes of $JKAP^{fl/fl}CD4^{Cre}$ mice,

whereas Th2 cells were not affected. In addition, the protein levels in the serum and mRNA levels in the aorta of the cytokines specifically released by these Th cells showed similar trends. These findings were consistent with our *in vitro* findings. The increased levels of IFN-γ, IL-4, and IL-17A mRNA in the aortic root also implied that Th cell infiltration was elevated in atherosclerosis in $JKAP^{fl/fl}CD4^{Cre}$ mice. Third, the level of proinflammatory cytokines was increased in $JKAP^{fl/fl}CD4^{Cre}$ mice, possibly due to conditional JKAP ablation in $CD4^+$ T cells promoting Th1 and Th17 cell polarization and thus increasing inflammation in the aorta[21, 23, 46]. Fourth, the ERK and NF-κB pathways were activated in the aortas of $JKAP^{fl/fl}CD4^{Cre}$ mice, which is also in line with our *in vitro* findings. Fifth, total cholesterol and LDL-cholesterol levels were higher in $JKAP^{fl/fl}CD4^{Cre}$ mice than control mice, which might result from the following: (i) JKAP deletion promoted $CD4^+$ T cells towards Th1 and Th17 differentiation to regulate immunity, which is closely related to the cholesterol level[47, 48]. In addition, the polarization of Th1 or Th17 cells increased the secretion of pro-inflammatory cytokines, such as IFN-γ and IL-17A, while the latter is considered to promote cholesterol levels[49, 50]. (ii) JKAP deletion directly activates TCR signaling[21], and TCR signaling involves the PI3K-Akt, MAPK, NF-κB, and calcium signaling pathways (www.kegg.jp/pathway/map04660), the latter of which are important for cholesterol production or metabolism. (iii) It was previously observed that JAKP (DUSP22) deletion particularly exacerbated lipid accumulation via its interaction with focal adhesion kinase (FAK)[51]. (iv) The relationship between JKAP, $CD4^+$ T cells, the ERK pathway, and the NF-κB pathway discovered in the current study might explain the effect of JKAP deletion on cholesterol levels to some extent. In addition, we hypothesized that the elevated cholesterol level contributed to the effect of JKAP deletion on facilitating the atherosclerosis process.

However, whether or not JKAP affects atherosclerosis using other approaches should be further explored. Furthermore, the experimental samples in this study were too small to draw a solid conclusion, which is another limitation of this study; further validation with larger experimental samples is needed in the future.

Conclusion

In conclusion, JKAP deficiency accelerates atherosclerosis progression by inducing Th1 and 17 polarization and inflammation in an ERK- and NF-κB pathway-dependent manner.

Funding

This research was funded by the Fujian Provincial Health and Family Planning Young and Midde-aged Key Members Talent Training Project (grant number 2017-ZQN-9) and the Fujian Provincial Natural Science Funding Project (grant number 2018J01244).

Declaration of Competing Interest

The authors declare that they have no known competing financial interests or personal relationships that could have influenced the work reported in this study.

References

1) Gupta K, Baloch F, Kakar TS, Agarwal H, Rawlley B, Khan UI, Iqbal R, Barolia R and Virani SS: The Pandemic of Coronary Heart Disease in South Asia: What Clinicians Need to Know. Curr Atheroscler Rep, 2023; 25: 359-372
2) Shaya GE, Leucker TM, Jones SR, Martin SS and Toth PP: Coronary heart disease risk: Low-density lipoprotein and beyond. Trends Cardiovasc Med, 2022; 32: 181-194
3) Fan J and Watanabe T: Atherosclerosis: Known and unknown. Pathol Int, 2022; 72: 151-160
4) Tsao CW, Aday AW, Almarzooq ZI, Anderson CAM, Arora P, Avery CL, Baker-Smith CM, Beaton AZ, Boehme AK, Buxton AE, Commodore-Mensah Y, Elkind MSV, Evenson KR, Eze-Nliam C, Fugar S, Generoso G, Heard DG, Hiremath S, Ho JE, Kalani R, Kazi DS, Ko D, Levine DA, Liu J, Ma J, Magnani JW, Michos ED, Mussolino ME, Navaneethan SD, Parikh NI, Poudel R, Rezk-Hanna M, Roth GA, Shah NS, St-Onge MP, Thacker EL, Virani SS, Voeks JH, Wang NY, Wong ND, Wong SS, Yaffe K, Martin SS, American Heart Association Council on E, Prevention Statistics C and Stroke Statistics S: Heart Disease and Stroke Statistics-2023 Update: A Report From the American Heart Association. Circulation, 2023; 147: e93-e621
5) Libby P: The changing landscape of atherosclerosis. Nature, 2021; 592: 524-533
6) Jebari-Benslaiman S, Galicia-Garcia U, Larrea-Sebal A, Olaetxea JR, Alloza I, Vandenbroeck K, Benito-Vicente A and Martin C: Pathophysiology of Atherosclerosis. Int J Mol Sci, 2022; 23: 3346
7) Xu S, Ilyas I, Little PJ, Li H, Kamato D, Zheng X, Luo S, Li Z, Liu P, Han J, Harding IC, Ebong EE, Cameron SJ, Stewart AG and Weng J: Endothelial Dysfunction in Atherosclerotic Cardiovascular Diseases and Beyond: From Mechanism to Pharmacotherapies. Pharmacol Rev, 2021; 73: 924-967
8) Pan W, Jie W and Huang H: Vascular calcification: Molecular mechanisms and therapeutic interventions. MedComm (2020), 2023; 4: e200
9) Ricciardi RM, Cipollone A, D'Ardes D, Di Giacomo D, Pignatelli P, Cipollone F, Curia MC, Magni P and Bucci M: Risk Factors and Immunoinflammatory Mechanisms

Leading to Atherosclerosis: Focus on the Role of Oral Microbiota Dysbiosis. Microorganisms, 2023; 11:
10) Guo Z, Wang L, Liu H and Xie Y: Innate Immune Memory in Monocytes and Macrophages: The Potential Therapeutic Strategies for Atherosclerosis. Cells, 2022; 11:
11) Hutton M, Frazer M, Lin A, Patel S and Misra A: New Targets in Atherosclerosis: Vascular Smooth Muscle Cell Plasticity and Macrophage Polarity. Clin Ther, 2023;
12) Chen W, Schilperoort M, Cao Y, Shi J, Tabas I and Tao W: Macrophage-targeted nanomedicine for the diagnosis and treatment of atherosclerosis. Nat Rev Cardiol, 2022; 19: 228-249
13) Wang J, Kang Z, Liu Y, Li Z, Liu Y and Liu J: Identification of immune cell infiltration and diagnostic biomarkers in unstable atherosclerotic plaques by integrated bioinformatics analysis and machine learning. Front Immunol, 2022; 13: 956078
14) Wei N, Xu Y, Li Y, Shi J, Zhang X, You Y, Sun Q, Zhai H and Hu Y: A bibliometric analysis of T cell and atherosclerosis. Front Immunol, 2022; 13: 948314
15) Saigusa R, Winkels H and Ley K: T cell subsets and functions in atherosclerosis. Nat Rev Cardiol, 2020; 17: 387-401
16) Wang Q, Wang Y and Xu D: Research progress on Th17 and T regulatory cells and their cytokines in regulating atherosclerosis. Front Cardiovasc Med, 2022; 9: 929078
17) Gistera A and Hansson GK: The immunology of atherosclerosis. Nat Rev Nephrol, 2017; 13: 368-380
18) Hinkley H, Counts DA, VonCanon E and Lacy M: T Cells in Atherosclerosis: Key Players in the Pathogenesis of Vascular Disease. Cells, 2023; 12:
19) Chen J, Xiang X, Nie L, Guo X, Zhang F, Wen C, Xia Y and Mao L: The emerging role of Th1 cells in atherosclerosis and its implications for therapy. Front Immunol, 2022; 13: 1079668
20) Yang G and Qiu Y: Effects of amlodipine combined with atorvastatin on Th17/Treg imbalance and vascular microcirculation in hypertensive patients with atherosclerosis: A double-blind, single-center randomized controlled trial. Medicine (Baltimore), 2023; 102: e32384
21) Li JP, Yang CY, Chuang HC, Lan JL, Chen DY, Chen YM, Wang X, Chen AJ, Belmont JW and Tan TH: The phosphatase JKAP/DUSP22 inhibits T-cell receptor signalling and autoimmunity by inactivating Lck. Nat Commun, 2014; 5: 3618
22) Li JP, Fu YN, Chen YR and Tan TH: JNK pathway-associated phosphatase dephosphorylates focal adhesion kinase and suppresses cell migration. J Biol Chem, 2010; 285: 5472-5478
23) Zhou R, Chang Y, Liu J, Chen M, Wang H, Huang M, Liu S, Wang X and Zhao Q: JNK Pathway-Associated Phosphatase/DUSP22 Suppresses CD4(+) T-Cell Activation and Th1/Th17-Cell Differentiation and Negatively Correlates with Clinical Activity in Inflammatory Bowel Disease. Front Immunol, 2017; 8: 781
24) Zhou X and Li M: JKAP serves as a potential biomarker for the evaluation of inflammatory condition, disease activity, and treatment response to TNF inhibitor in ankylosing spondylitis patients. Mod Rheumatol, 2022; 32: 613-618
25) Wang C, Huo H, Li J, Zhang W, Liu C, Jin B, Wang H and Zhao P: The longitudinal changes of serum JKAP and IL-17A, and their linkage with anxiety, depression, and cognitive impairment in acute ischemic stroke patients. J Clin Lab Anal, 2022; 36: e24762
26) Zeng J, Liu J, Qu Q, Zhao X and Zhang J: JKAP, Th1 cells, and Th17 cells are dysregulated and inter-correlated, among them JKAP and Th17 cells relate to cognitive impairment progression in Alzheimer's disease patients. Ir J Med Sci, 2022; 191: 1855-1861
27) Gao W, Gao L, Yang F and Li Z: Circulating JNK pathway-associated phosphatase: A novel biomarker correlates with Th17 cells, acute exacerbation risk, and severity in chronic obstructive pulmonary disease patients. J Clin Lab Anal, 2022; 36: e24153
28) Wu R, Zeng J, Yuan J, Deng X, Huang Y, Chen L, Zhang P, Feng H, Liu Z, Wang Z, Gao X, Wu H, Wang H, Su Y, Zhao M and Lu Q: MicroRNA-210 overexpression promotes psoriasis-like inflammation by inducing Th1 and Th17 cell differentiation. J Clin Invest, 2018; 128: 2551-2568
29) Brauner S, Jiang X, Thorlacius GE, Lundberg AM, Ostberg T, Yan ZQ, Kuchroo VK, Hansson GK and Wahren-Herlenius M: Augmented Th17 differentiation in Trim21 deficiency promotes a stable phenotype of atherosclerotic plaques with high collagen content. Cardiovasc Res, 2018; 114: 158-167
30) Zeng Z, Xu J and Zheng W: Artemisinin protects PC12 cells against beta-amyloid-induced apoptosis through activation of the ERK1/2 signaling pathway. Redox Biol, 2017; 12: 625-633
31) Li X, Dong L, Liu J, Wang C, Zhang Y, Mei Q, Han W, Xie P and Nie J: Low-Dose Decitabine Augments the Activation and Anti-Tumor Immune Response of IFN-gamma(+) CD4(+) T Cells Through Enhancing IkappaBalpha Degradation and NF-kappaB Activation. Front Cell Dev Biol, 2021; 9: 647713
32) Lacy M, Burger C, Shami A, Ahmadsei M, Winkels H, Nitz K, van Tiel CM, Seijkens TTP, Kusters PJH, Karshovka E, Prange KHM, Wu Y, Brouns SLN, Unterlugauer S, Kuijpers MJE, Reiche ME, Steffens S, Edsfeldt A, Megens RTA, Heemskerk JWM, Goncalves I, Weber C, Gerdes N, Atzler D and Lutgens E: Cell-specific and divergent roles of the CD40L-CD40 axis in atherosclerotic vascular disease. Nat Commun, 2021; 12: 3754
33) Zhang L, Wang T, Wang XQ, Du RZ, Zhang KN, Liu XG, Ma DX, Yu S, Su GH, Li ZH, Guan YQ and Du NL: Elevated frequencies of circulating Th22 cell in addition to Th17 cell and Th17/Th1 cell in patients with acute coronary syndrome. PLoS One, 2013; 8: e71466
34) Flego D, Severino A, Trotta F, Previtero M, Ucci S, Zara C, Pedicino D, Massaro G, Biasucci LM, Liuzzo G and Crea F: Altered CD31 expression and activity in helper T cells of acute coronary syndrome patients. Basic Res Cardiol, 2014; 109: 448
35) Marchini T, Hansen S and Wolf D: ApoB-Specific CD4(+) T Cells in Mouse and Human Atherosclerosis. Cells, 2021; 10:
36) Filatova AY, Pylaeva EA, Potekhina AV, Ruleva NY,

Klesareva EA, Radyukhina NV, Masenko VP, Shchinova AM, Noeva EA, Provatorov SI, Afanas'eva OI and Aref'eva TI: Low Blood Content of IL-10-Producing CD4(+) T Cells as a Risk Factor for Progression of Coronary Atherosclerosis. Bull Exp Biol Med, 2019; 166: 330-333
37) Wang Y, Li W, Zhao T, Zou Y, Deng T, Yang Z, Yuan Z, Ma L, Yu R, Wang T and Yu C: Interleukin-17-Producing CD4(+) T Cells Promote Inflammatory Response and Foster Disease Progression in Hyperlipidemic Patients and Atherosclerotic Mice. Front Cardiovasc Med, 2021; 8: 667768
38) Zhou L, Long J, Sun Y, Chen W, Qiu R and Yuan D: Resveratrol ameliorates atherosclerosis induced by high-fat diet and LPS in ApoE(-/-) mice and inhibits the activation of CD4(+) T cells. Nutr Metab (Lond), 2020; 17: 41
39) Lu S, Deng J, Liu H, Liu B, Yang J, Miao Y, Li J, Wang N, Jiang C, Xu Q, Wang X and Feng J: PKM2-dependent metabolic reprogramming in CD4(+) T cells is crucial for hyperhomocysteinemia-accelerated atherosclerosis. J Mol Med (Berl), 2018; 96: 585-600
40) Yang Q, Zhuang J, Cai P, Li L, Wang R and Chen Z: JKAP relates to disease risk, severity, and Th1 and Th17 differentiation in Parkinson's disease. Ann Clin Transl Neurol, 2021; 8: 1786-1795
41) Gaud G, Lesourne R and Love PE: Regulatory mechanisms in T cell receptor signalling. Nat Rev Immunol, 2018; 18: 485-497
42) Watson SR, Cooper KM, Liu P, Gharraee N, Du L, Han SM, Pena EA, Sutton MA, Eberth JF and Lessner SM: Diet alters age-related remodeling of aortic collagen in mice susceptible to atherosclerosis. Am J Physiol Heart Circ Physiol, 2021; 320: H52-H65
43) Zhang Y, Ying F, Tian X, Lei Z, Li X, Lo CY, Li J, Jiang L and Yao X: TRPM2 Promotes Atherosclerotic Progression in a Mouse Model of Atherosclerosis. Cells, 2022; 11:
44) Oberkersch R, Maccari F, Bravo AI, Volpi N, Gazzaniga S and Calabrese GC: Atheroprotective remodelling of vascular dermatan sulphate proteoglycans in response to hypercholesterolaemia in a rat model. Int J Exp Pathol, 2014; 95: 181-190
45) Ouerd S, Idris-Khodja N, Trindade M, Ferreira NS, Berillo O, Coelho SC, Neves MF, Jandeleit-Dahm KA, Paradis P and Schiffrin EL: Endothelium-restricted endothelin-1 overexpression in type 1 diabetes worsens atherosclerosis and immune cell infiltration via NOX1. Cardiovasc Res, 2021; 117: 1144-1153
46) Taleb S: Inflammation in atherosclerosis. Arch Cardiovasc Dis, 2016; 109: 708-715
47) Yero A, Bouassa RM, Ancuta P, Estaquier J and Jenabian MA: Immuno-metabolic control of the balance between Th17-polarized and regulatory T-cells during HIV infection. Cytokine Growth Factor Rev, 2023; 69: 1-13
48) Schulte S, Sukhova GK and Libby P: Genetically programmed biases in Th1 and Th2 immune responses modulate atherogenesis. Am J Pathol, 2008; 172: 1500-1508
49) Varshney P and Saini N: PI3K/AKT/mTOR activation and autophagy inhibition plays a key role in increased cholesterol during IL-17A mediated inflammatory response in psoriasis. Biochim Biophys Acta Mol Basis Dis, 2018; 1864: 1795-1803
50) Saggini A, Anogeianaki A, Maccauro G, Tete S, Salini V, Caraffa A, Conti F, Fulcheri M, Galzio R and Shaik-Dasthagirisaheb YB: Cholesterol, cytokines and diseases. Int J Immunopathol Pharmacol, 2011; 24: 567-581
51) Ge C, Tan J, Dai X, Kuang Q, Zhong S, Lai L, Yi C, Sun Y, Luo J, Zhang C, Zhu L, Wang B and Xu M: Hepatocyte phosphatase DUSP22 mitigates NASH-HCC progression by targeting FAK. Nat Commun, 2022; 13: 5945

Supplementary Table 1. Primer sequences

Gene	Forward primer (5'->3')	Reverse primer (5'->3')
JKAP	GCCAGGCCTATGTTGGAGGGAGTT	TGTATGCGATCACCAGTGTCAC
IFNG	AGACAATCAGGCCATCAGCA	CAACAGCTGGTGGACCACTC
IL4	GGTCACAGGAGAAGGGACGCC	TGCGAAGCACCTTGGAAGCCC
IL17A	CAACAGCTGGTGGACCACTC	CAACAGCTGGTGGACCACTC
GAPDH	GAGTCCACTGGCGTCTTCAC	ATCTTGAGGCTGTTGTCATACTTCT

Supplementary Table 2. Antibodies information of western blot and immunohistochemistry used in this study

Antibody	Company	Dilution (western blot / immunohistochemistry)
Anti-JKAP antibody	Abcam (USA)	1:1000/1:200
Anti-ERK antibody	Affinity (China)	1:1000
Anti-p-ERK antibody	Affinity (China)	1:1000/1:200
Anti-p38 antibody	Affinity (China)	1:1000/-
Anti-p-p38 antibody	Affinity (China)	1:1000/1:200
Anti-JNK antibody	Affinity (China)	1:1000/-
Anti-p-JNK antibody	Affinity (China)	1:1000/1:200
Anti-IκBα antibody	Affinity (China)	1:1000/-
Anti-p-IκBα antibody	Affinity (China)	1:1000/1:200
Anti-CD68 antibody	Santa Cruz (USA)	-/1:100
Anti-α-SMA antibody	Abcam (USA)	-/1:200
Anti-CD4 antibody	Santa Cruz (USA)	-/1:100
Anti-TNF-α antibody	Affinity (China)	-/1:200
Anti-IL-6 antibody	Affinity (China)	-/1:200
Anti-IFN-γ antibody	Affinity (China)	-/1:200
Anti-IL-4 antibody	Affinity (China)	-/1:200
Anti-IL-17A antibody	Affinity (China)	-/1:200
Anti-GAPDH antibody	Abcam (USA)	1:5000/-
Goat Anti-Rabbit IgG HRP	Abcam (USA)	1:10000/1:1000

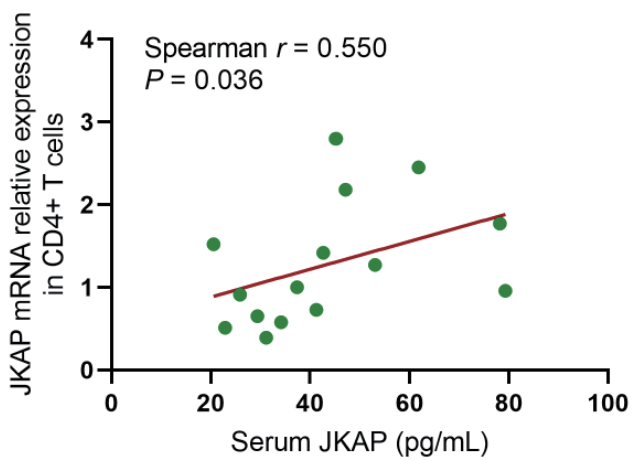

Supplementary Fig. 1. The correlation between serum JKAP level and JKAP relative expression in $CD4^+$ T cells in CHD patients

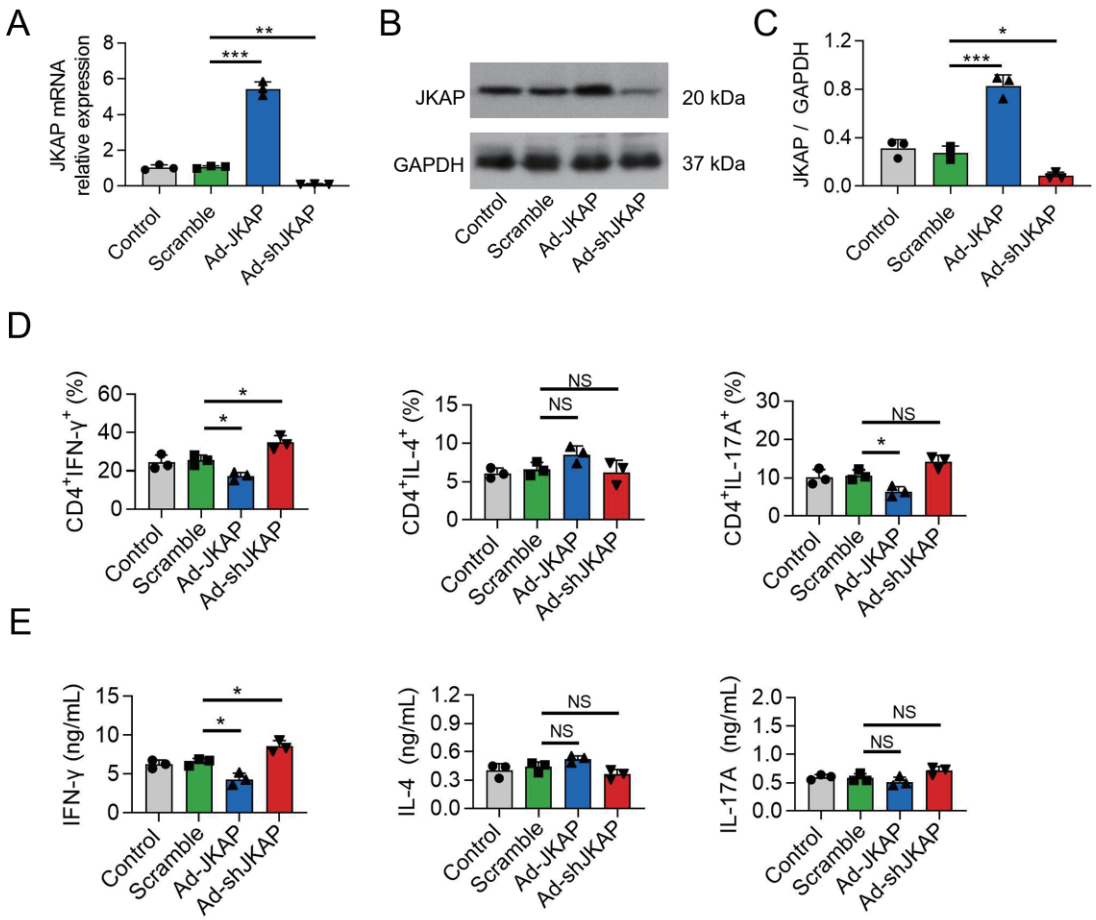

Supplementary Fig. 2. The effect of JKAP modification on Th cell polarization from normal control naïve $CD4^+$ T cells

The comparison of JKAP mRNA expression ($n=3$) (A) and protein expression ($n=3$) (B, C); the comparison of Th1 cells, Th2 cells and Th17 cells ($n=3$) (D); the comparison of IFN-γ, IL-4 and IL-17A levels ($n=3$) (E) after transfection in normal control naïve $CD4^+$ T cells. NS: not significant; * $P<0.05$; **: $P<0.01$; *** $P<0.001$. The bars represent the mean values, and error bars represent the standard deviations.

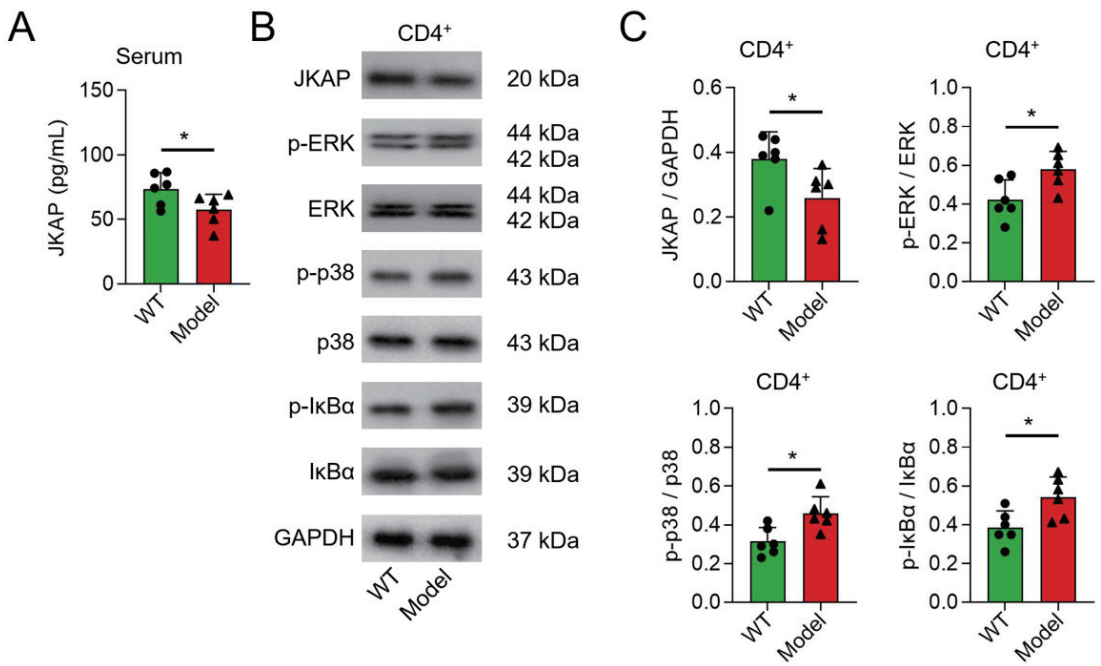

Supplementary Fig. 3. JKAP, p-ERK, p-p38 and p-IκBα in atherosclerotic mice (Model) and normal mice (WT)

The serum JKAP level in Model mice and WT mice ($n=6$) (A), expressions of JKAP, p-ERK, p-p38 and p-IκBα in CD4$^+$ T cells from blood samples between Model mice and WT mice ($n=6$) (B-C). * $P<0.05$. The bars represent the mean values, and error bars represent the standard deviations.

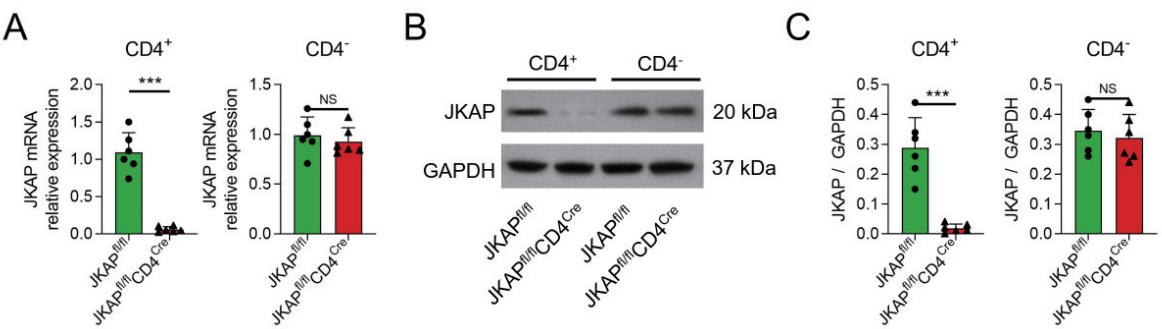

Supplementary Fig. 4. Verification of JKAP$^{fl/fl}$CD4^{Cre} mouse construction

The comparison of JKAP mRNA expression (A) and protein expression (C, D) in CD4$^+$ T cells ($n=6$) and CD4$^-$ T cells ($n=6$). NS: not significant; ***: $P<0.001$. The bars represent the mean values, and error bars represent the standard deviations.

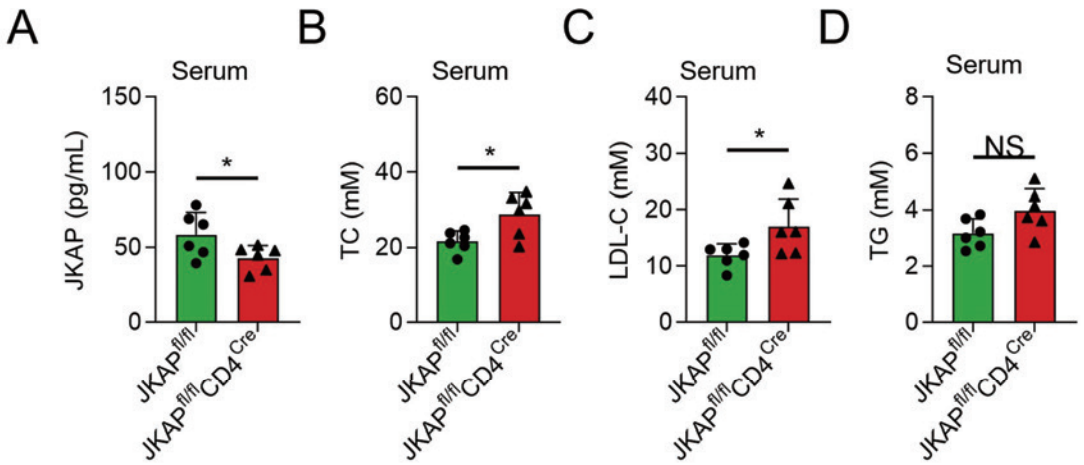

Supplementary Fig. 5. Blood JKAP, TC, LDL-C and TG in JKAP$^{fl/fl}$CD4^{Cre} mice

The comparison of the serum JKAP level ($n=6$) (A), serum TC level ($n=6$) (B), serum LDL-C level ($n=6$) (C), and serum TG level ($n=6$) (D) between the JKAP$^{fl/fl}$CD4^{Cre} and JKAP$^{fl/fl}$ mouse groups. NS: not significant; * $P<0.05$. The bars represent the mean values, and error bars represent the standard deviations.

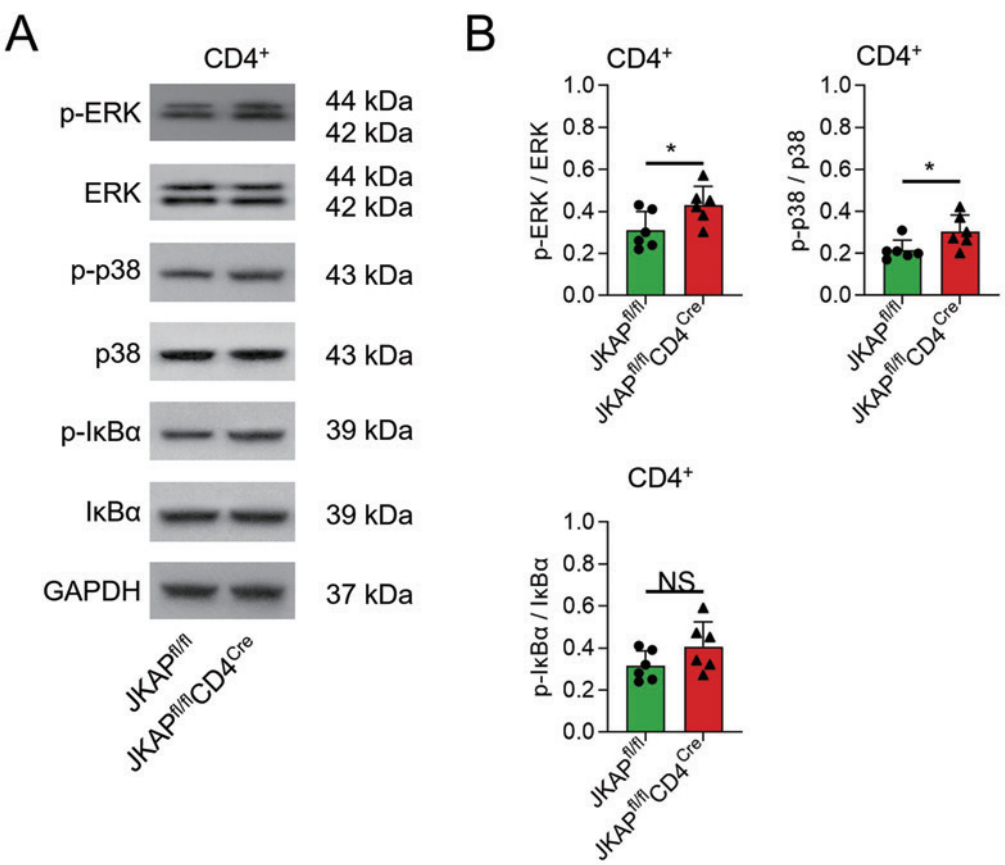

Supplementary Fig. 6. p-ERK, p-p38 and p-IκBα in CD4$^+$ T cells from atherosclerotic lesions

Western blot images of p-ERK ($n=6$), p-p38 ($n=6$) and p-IκBα ($n=6$) in CD4$^+$ T cells from atherosclerotic lesion between the JKAP$^{fl/fl}$ CD4^{Cre} and JKAP$^{fl/fl}$ mouse groups (A), and the comparison of corresponding quantifications (B). NS: not significant; *: $P<0.05$. The bars represent the mean values, and error bars represent the standard deviations.